Intermittent chaos in dense gaseouslike media driven by coupling cross thermodiffusive effects

Stefano A. Mezzasalma

IISM, Materials Science and Engineering Institute, University of Genoa, Corso Perrone 24A, I-16161 Genova, Italy

Andrea Mazzino

INFM, Department of Physics, University of Genoa, Via Dodecaneso 33, I-16146 Genova, Italy

Intermittent chaotic behavior induced by a thermodiffusive coupling is investigated by analysis of a five-mode (Lorenz-like) truncated model describing a binary, diluted solution which behaves as a gaslike system. The obtained nonlinear equations coherently agree with the marginal stability locus point when the absence of a stationary state for the mass transfer is considered. For a wide range of reduced Rayleigh number values r, we show that the truncated model exhibits the Pomeau-Manneville intermittency route to chaos when the control (Soret-based) phenomenological coefficient $\langle \delta \rangle$ approaches some critical values $\langle \delta \rangle_c$. Numerical simulations evaluating the generalized Lyapunov exponent against the control parameter displacement close to the intermittency threshold, $L(1)$ vs $(\langle \delta \rangle_c - \langle \delta \rangle)$, are reported inside the chaotic region. The achieved results agree reasonably with theoretical predictions. [S1063-651X(97)12112-2]

INTRODUCTION

The importance of ''transverse'' (Soret cross) effects, although consisting of a weak coupling between thermal gradient and mass flux, has been henceforth recognized in several physicochemical phenomena [1,2]. Soret gradients in solids [3] (especially alloys and metals; see also electrical cross-phenomena [4]) have been investigated by measurements of the heat of transport [as well as of (inter)diffusion coefficients] of different atomic species in diffusion and self-diffusion phenomena occurring in a crystal lattice [3,5]. More recently, by a sort of ''background'' internal friction, which has been interpreted according to point-defect relaxations driven by nonlinear thermal cross-effects [6], there are reasons to believe that Soret-like transverse contributions could play a primary role in some fields of material science. In a liquid (mixture) [7,8], as the thermal diffusivity χ is much larger than the diffusion coefficient D, the temperature fluctuations can be neglected, and Soret gradient-induced effects are usually dealt with by taking advantage of the stationary state for the mass transfer, i.e., $\boldsymbol{J}_1 = 0$ [9,10]. This condition is a constraint to be considered in developing a classical linear analysis of the stability and in writing any related truncated model [11]. In the present case, since $\chi/D \gg 1$ [9,12], the aforesaid constraint for the mass flux cannot be used, and a simple recast of the linear stability analysis is required. Accordingly, in a nonstationary state, thermal and diffusive Lorenz-like dynamics are expected to be coupled by a transverse (Soret) coefficient [11]. Moreover, in a gaseouslike system, this cross-contribution is greater than in liquids and/or solids and, in principle, appreciably depends on temperature [9,12].

In this paper, intermittency induced by transverse Soret-based gradients has been attempted for a dense gaslike medium, whose dynamics is described by a nonlinear five-mode Lorenz-like model. As usual, deterministic equations are obtained by a severe truncation of a modal expansion of the governing finite amplitude convection [13] in a binary diluted gaslike solution heated from below, and in the presence of a concentration gradient [14].

It is known that large systems of nonlinear coupled maps (the so-called coupled map lattices) [15] are the simplest models exhibiting alternation between turbulent and laminar regions in space, which is usually denoted as *spatiotemporal intermittency*. This type of coupled map lattice is constructed (as, for example, the ones introduced by Chaté and Manneville [16,17]) by coupling together maps exhibiting both chaotic and laminar states. The mechanism leading to intermittency [18] is due to the (coupling induced) interplay between laminar and turbulent regions. Roughly speaking, the trajectory ''absorbed'' in some laminar states may be pulled back into chaotic regions thank to (coupling) interactions between maps. Without coupling, the laminar states are ''fully absorbing'' (i.e., the trajectory cannot return into a chaotic state).

Here our major goal will be to show that, for our nonlinear five-mode truncated model, a role of the coupling Soret-based gradient is to drive the system (just as in the coupled map lattices) from stable laminar motion into intermittent chaotic motion (or vice versa).

Taking the cross-term as the control parameter, the model exhibits the well defined routes to chaos, originally proposed for the Lorenz 1963 model (hereafter $L63$) by Manneville and Pomeau [19], namely, the so called *tangent bifurcation intermittency*. In the intermittent region, the regular (laminar) behavior is ''randomly'' disrupted by a ''burst'' of chaoticity of finite duration, after which a new laminar phase takes place, and so on. The instability leading to the burst is due to the fact that the modulus of at least one Floquet multiplier [20] crosses the unit circle along the real axis at $+1$.

Results will be reported relative to the transition occurring at the critical control parameter value ~ 0.0955, provided with a reduced Rayleigh number $r \sim 167$. Indeed, as we shall see, the system also exhibits tangent bifurcation intermittency for smaller r values.

In order to capture the influence of fluctuations on the

system ''predictability'' close to the intermittency threshold, we shall employ results following from the general thermodynamical theory of dynamical systems which lead to the definition of generalized Lyapunov exponents $L(q)$. Accordingly, a reasonable definition of the predictability time of the system, which takes into account fluctuations, can be given. In the intermittent region, an inverse predicatability time will be derived numerically, and compared with theoretical results based on renormalization argument [21].

I. MARGINAL LOCUS OF STABILITY

Consider the Soret cross-effect occurring in a gaslike, binary, and diluted solution [9–11]. The starting phenomenological equations are of the forms [1,2]:

$$\mathbf{J}'_q = -K\nabla T,$$

$$\mathbf{J}_1 = -\rho c_1(1-c_1)D'\nabla T - \rho D\nabla c_1, \tag{1}$$

where T is the temperature, c_1 is the mole fraction of one of two components, ρ is the density, $\mathbf{J}'_q$ is the thermal flux including the enthalpy transport, $\mathbf{J}_1$ is the matter flux due to c_1, and K, D, and D' are the Fourier, Fick, and Soret coefficients, respectively. The applied equations consist of the usual balance and state equations [1].

As the stationary equilibrium condition for the mass flux does not apply, namely, $\mathbf{J}_1 \neq \mathbf{0}$, from application of the linear analysis to the stability of infinitesimal disturbances [2,7,13], and some algeabric passages, the marginal stability locus point becomes

$$(1+\langle\delta\rangle)\mathsf{R}-\bar{\mathsf{R}}=\tfrac{27}{4}\pi^4,$$

$$\frac{\bar{P}^2}{(1+\bar{P})(P+\bar{P})}\left[1+\frac{P}{\bar{P}}\frac{\langle\delta\rangle}{(1+P)}\right]\mathsf{R}-\frac{P^2}{(1+P)(P+\bar{P})}\bar{\mathsf{R}}$$
$$=\tfrac{27}{4}\pi^4, \tag{2}$$

where R and $\bar{\mathsf{R}}$ are the thermal and solutal Rayleigh numbers, P and $\bar{P}$ are the Prandtl and Schmidt numbers and the Soret-based contribution $\langle\delta\rangle=S_T(\gamma_m/\alpha_P)\langle\widetilde{c_1}\rangle(1-\langle\widetilde{c_1}\rangle)$ contains the thermal and mass expansivities α_P and γ_m together with the contribution of vertical concentration profile, which is approximated to its mean value, i.e., $\widetilde{c}_1\simeq\langle\widetilde{c}_1\rangle$ [10].

The Soret coefficient $S_T=D'/D$ coherently introduces the contribution of the temperature gradient into the mass flux $\mathbf{J}_1$. In fact, when $S_T>0$, from analytical expressions for the marginal stability locus point (2), it may be observed that in the $\mathsf{R}>0$ half-plane, corresponding to positive (destabilizing) temperature gradient, we have an increase in the unstable region; conversely, for $\mathsf{R}<0$, the stable region increases. Accordingly, the intersection point of the stationary and oscillatory marginal stability locus in the thermohaline convection, which is $\mathbf{T}=(\bar{\mathsf{R}}_T,\mathsf{R}_T)$ where $\bar{\mathsf{R}}_T=\tfrac{27}{4}\pi^4[(1+P)/(P-P)]$, and $\mathsf{R}_T=\tfrac{27}{4}\pi^4[(1+\bar{P})/(\bar{P}-P)]$, in the case when the Soret effect moves to the point $\mathbf{S}=(\bar{\mathsf{R}}_S,\mathsf{R}_S)$, being now

$$\bar{\mathsf{R}}_S=\frac{27}{4}\pi^4\frac{1+P+A_{P\bar{P}}\langle\delta\rangle}{\bar{P}-P-B_{P\bar{P}}\langle\delta\rangle},$$

$$\mathsf{R}_S=\frac{27}{4}\pi^4\frac{1+\bar{P}}{\bar{P}-P-B_{P\bar{P}}\langle\delta\rangle}, \tag{3}$$

where $A_{P\bar{P}}=[P(1+\bar{P})1+P+\bar{P}]+\bar{P}(1+\bar{P}-P)]/[P\bar{P}+P+\bar{P}]$ and $B_{P\bar{P}}=[P(P\bar{P}+P-\bar{P})/P\bar{P}+P+\bar{P}]$.

All mathematical details which, starting from the thermohaline problem, lead to Eq. (2) (as well as the investigation of stability and/or instability transitions predicted by the locus point) are not important here. In fact, they follow directly from the linear analysis applied to the stability of infinitesimal disturbances near the mechanical (pure conductive) equilibrium. Nevertheless, a summary of the most important steps is reported in Appendixes A and B. The proof of validity of marginal equations (2) will be given in Sec. II, where we show the agreement with the linear theory results following from the linearization of the involved deterministic model.

II. TRUNCATED MODEL

As in the $L63$ model (see Ref. [22] and Appendix C), one can approximate the nondimensional stream function $\bar{\psi}$, and temperature and mass concentration $\bar{\theta}$ and $\bar{\xi}$, with

$$\bar{\psi}\simeq\frac{(\alpha^2+\pi^2)}{\pi\alpha}\sqrt{2}X_1\sin(\alpha\mathcal{X})\sin(\pi\mathcal{Z}),$$

$$\bar{\theta}\simeq\epsilon\frac{R_1(\alpha)}{\pi}[\sqrt{2}X_2\cos(\alpha\mathcal{X})\sin(\pi\mathcal{Z})-X_3\sin(2\pi\mathcal{Z})], \tag{4}$$

$$\bar{\xi}\simeq\bar{\epsilon}\frac{R_1(\alpha)}{\pi}[\sqrt{2}X_4\cos(\alpha\mathcal{X})\sin(\pi\mathcal{Z})-X_5\sin(2\pi\mathcal{Z})],$$

where X_i's are related to the coefficients of the Fourier development, $\mathcal{X}$ and $\mathcal{Z}$ are nondimensional spatial coordinates, α is a non-dimensional wave number, R_1 is the marginal stability α locus in the Bénard problem, and $\epsilon=\Delta\widetilde{T}/|\Delta\widetilde{T}|=\pm1$ together with $\bar{\epsilon}=\Delta\widetilde{c}_1/|\Delta\widetilde{c}_1|=\pm1$ determine the quadrant of the $(\bar{R},R)$ plane. A comparison between the original Fourier series (see Appendix C) and Eqs. (4) allows a relationship between the X_i coefficients and the real and imaginary parts of the Fourier amplitudes to be written as $X_1=2\sqrt{2}\pi[\alpha/R_1(\alpha)]^{1/3}\bar{\Psi}_{1,1}^{(1)}$, $X_2=\epsilon[2\sqrt{2}\pi/R_1(\alpha)]\bar{\Theta}_{1,1}^{(2)}$, $X_3=\epsilon[2\pi/R_1(\alpha)]\bar{\Theta}_{0,2}^{(2)}$, $X_4=\bar{\epsilon}[R_1(\alpha)/2\sqrt{2}\pi]\bar{\Gamma}_{1,1}^{(2)}$, and $X_5=\bar{\epsilon}[R_1(\alpha)/2\pi]\bar{\Gamma}_{0,2}^{(2)}$.

After substituting Eq. (4) into the governing physical system [Eq. (C1) in Appendix C] and introducing the adimensional ''reduced'' quantities $r(\alpha)=R/R_1(\alpha)$, $\bar{r}(\alpha)=\bar{R}/R_1(\alpha)$, and $b(\alpha)=4\pi^2/(\pi^2+\alpha^2)$, by applying the Galerkin procedure [23] one arrives at

$$\dot{X}_1 = -P\left(X_1 - \epsilon X_2 + \epsilon\frac{P}{\bar{P}}X_4\right),$$

$$\dot{X}_2 = -X_1 X_3 + \epsilon r X_1 - X_2,$$

$$\dot{X}_3 = X_1 X_2 - b X_3, \tag{5}$$

$$\dot{X}_4 = -X_1 X_5 + \bar{\epsilon}\,\bar{r}X_1 - \epsilon\bar{\epsilon}\langle\delta\rangle X_2 - \frac{P}{\bar{P}}X_4,$$

$$\dot{X}_5 = X_1 X_4 - b\left(\epsilon\bar{\epsilon}\langle\delta\rangle X_3 + \frac{P}{\bar{P}}X_5\right).$$

Obviously, when the Soret cross-term is neglected and $\epsilon = -\bar{\epsilon} = 1$ Eqs. (5) reduce to a five-mode truncated model for the thermohaline convection [10,14], with temperature and concentration gradients acting oppositely.

Stationary states and stability

The components of the stationary states [24] are provided by

$$P X_{1S}(X_{1S}{}^4 + \mathcal{B}_\delta X_{1S}{}^2 + \mathcal{C}_\delta) = 0$$

$$\mathcal{B}_\delta = b[1 - r(1 - \beta_\epsilon\langle\delta\rangle)] + a(1+\bar{r}),$$
$$\mathcal{C}_\delta = ab[\bar{r} + 1 - r(1+\langle\delta\rangle)], \tag{6}$$

where $a = b(P/\bar{P})^2$ and $\beta_\epsilon = \epsilon(1 + P/\bar{P}) - 1$, and by

$$X_{2S} = \epsilon b r \frac{X_{1S}}{b + X_{1S}^2},$$

$$X_{3S} = \epsilon r \frac{X_{1S}^2}{b + X_{1S}^2},$$

$$X_{4S} = \bar{\epsilon}b\frac{P}{\bar{P}}\frac{X_{1S}}{b\left(\dfrac{P}{\bar{P}}\right)^2 + X_{1S}^2}\left\{\bar{r} + \frac{r}{b + X_{1S}^2}\langle\delta\rangle\right.$$
$$\left.\times\left[\beta_\epsilon\left(\frac{\bar{P}}{P}X_{1S}\right)^2 - b\right]\right\}, \tag{7}$$

$$X_{5S} = \bar{\epsilon}\frac{X_{1S}^2}{b\left(\dfrac{P}{\bar{P}}\right)^2 + X_{1S}^2}\left[\bar{r} - \epsilon b\frac{r}{b + X_{1S}^2}\langle\delta\rangle\left(1 + \frac{P}{\bar{P}}\right)\right],$$

so that $X_O \equiv 0$ is obviously stationary.

To obtain the other stationary points, it is necessary to solve the above biquadratic equation (6). To this end, in addition to $\mathcal{B}_\delta$ and $\mathcal{C}_\delta$, another important expression is given by the discriminant of Eq. (6), namely, $\Delta_\delta = \mathcal{B}_\delta^2 - 4\mathcal{C}_\delta > 0$. In particular, the equation $\Delta_\delta = 0$ is that of a simple parabola

with the vertex on the r axis which defines a region of the $(\bar{r}, r)$ plane where the solutions of Eq. (6) must be looked for. These are

$$(\text{I}) \quad X_{1S}^{(1)} = \frac{1}{\sqrt{2}}\sqrt{-\mathcal{B}_\delta + \sqrt{\Delta}_\delta},$$

$$X_{1S}^{(2)} = -\frac{1}{\sqrt{2}}\sqrt{-\mathcal{B}_\delta + \sqrt{\Delta}_\delta}, \tag{8}$$

$$(\text{II}) \quad X_{1S}^{(3)} = \frac{1}{\sqrt{2}}\sqrt{-\mathcal{B}_\delta - \sqrt{\Delta}_\delta},$$

$$X_{1S}^{(4)} = -\frac{1}{\sqrt{2}}\sqrt{-\mathcal{B}_\delta - \sqrt{\Delta}_\delta}.$$

Thus, defining $z = (1/\sqrt{2})\sqrt{-\mathcal{B}_\delta + \sqrt{\Delta}_\delta} \equiv X_{1S}^{(1)}$ and $y = (1/\sqrt{2})\sqrt{-\mathcal{B}_\delta - \sqrt{\Delta}_\delta} \equiv X_{1S}^{(3)}$, the four stationary solutions can be written as

$$X_S^{(1)} \equiv \begin{pmatrix} z \\ \epsilon b r\dfrac{z}{z^2+b} \\ \epsilon r\dfrac{z^2}{z^2+b} \\ \bar{\epsilon}b\bar{r}\dfrac{P}{\bar{P}}\dfrac{z}{z^2+a} \\ \bar{\epsilon}\bar{r}\dfrac{z^2}{z^2+a} \end{pmatrix}, \quad X_S^{(2)} \equiv \begin{pmatrix} -z \\ -\epsilon b r\dfrac{z}{z^2+b} \\ \epsilon r\dfrac{z^2}{z^2+b} \\ -\bar{\epsilon}b\bar{r}\dfrac{P}{\bar{P}}\dfrac{z}{z^2+a} \\ \bar{\epsilon}\bar{r}\dfrac{z^2}{z^2+a} \end{pmatrix}, \tag{9}$$

$$X_S^{(3)} \equiv \begin{pmatrix} y \\ \epsilon b r\dfrac{y}{y^2+b} \\ \epsilon r\dfrac{y^2}{y^2+b} \\ \bar{\epsilon}b\bar{r}\dfrac{P}{\bar{P}}\dfrac{y}{y^2+a} \\ \bar{\epsilon}\bar{r}\dfrac{y^2}{y^2+a} \end{pmatrix}, \quad X_S^{(4)} \equiv \begin{pmatrix} -y \\ -\epsilon b r\dfrac{y}{y^2+b} \\ \epsilon r\dfrac{y^2}{y^2+b} \\ -\bar{\epsilon}b\bar{r}\dfrac{P}{\bar{P}}\dfrac{y}{y^2+a} \\ \bar{\epsilon}\bar{r}\dfrac{y^2}{y^2+a} \end{pmatrix}. \tag{10}$$

Accordingly, with regard to Eqs. (6)–(10) and omitting the S indexes, one has $X_{3,5}^{(1)} = X_{3,5}^{(2)}$ and $X_{3,5}^{(3)} = X_{3,5}^{(4)}$, while $X_{1,2,4}^{(1)} = -X_{1,2,4}^{(2)}$ and $X_{1,2,4}^{(3)} = -X_{1,2,4}^{(4)}$. The domains of the pairs $X_S^{(1,2)}$ and $X_S^{(3,4)}$ in the $(\bar{r}, r)$ plane descend from the analysis of the aforesaid biquadratic equation (6), and are given, respectively, by the following conditions [16]:

$$\mathcal{D}_{12}^{(\delta)}=(\mathcal{B}_> \cup \mathcal{C}_<)\cap(\mathcal{B}_< \cup \Delta_>), \qquad (11)$$

$$\mathcal{D}_{34}^{(\delta)}=\mathcal{B}_< \cup \mathcal{C}_> \cup \Delta_>, \qquad (12)$$

where $\mathcal{A}_> \equiv \{(\bar{r},r):\mathcal{A}_\delta>0\}$ and $\mathcal{A}_< \equiv \{(\bar{r},r):\mathcal{A}_\delta<0\}$, $\mathcal{A}=\mathcal{B},\mathcal{C},\Delta$, while X_O is defined everywhere, that is, $\mathcal{D}_O \equiv \mathcal{R}^2$.

If $\mathcal{D}_{12}$ and $\mathcal{D}_{34}$ denote the domains of the above pairs in the absence of the Soret effect (thermohaline convection), if $S_T>0$ one has $\mathcal{D}_{12}^{(\delta)}\times\mathcal{D}_{34}^{(\delta)}\subset\mathcal{D}_{12}\times\mathcal{D}_{34}$ when $r>0$ ($\times$ is the Cartesian product), and $\mathcal{D}_{12}\subset\mathcal{D}_{12}^{(\delta)}$ when $r<0$, as can be reasonably expected from the results of the linear theory [see Eqs. (2)]. Contributions opposing to stability, coming from the signs of the two gradients, are also pointed out in the new expression for X_{5S}, the distortion of the stationary concentration profile, which decreases in the presence of the positive temperature gradient.

Indicating with $\widetilde{X}_i$ the coordinate components around a generic stationary solution, and setting $\widetilde{X}_i=X_{iS}+\delta x_i$, the linearized system in the perturbations δx_i is

$$\begin{pmatrix}\dot{\delta x}_1\\\dot{\delta x}_2\\\dot{\delta x}_3\\\dot{\delta x}_4\\\dot{\delta x}_5\end{pmatrix}=\begin{pmatrix}-P & \epsilon P & 0 & -\epsilon\dfrac{P^2}{\bar{P}} & 0\\[2mm]\epsilon(r-X_{3S}) & -1 & -X_{1S} & 0 & 0\\[2mm]X_{2S} & X_{1S} & -b & 0 & 0\\[2mm]\bar{\epsilon}(\bar{r}-X_{5S}) & -\epsilon\bar{\epsilon}\langle\delta\rangle & 0 & -\dfrac{P}{\bar{P}} & -X_{1S}\\[2mm]X_{4S} & 0 & -\epsilon\bar{\epsilon}b\langle\delta\rangle & X_{1S} & -b\dfrac{P}{\bar{P}}\end{pmatrix}\begin{pmatrix}\delta x_1\\\delta x_2\\\delta x_3\\\delta x_4\\\delta x_5\end{pmatrix}. \qquad (13)$$

The characteristic equation for X_O considers the Soret contribution only in the known term of a three-degree polynomial:

$$(\lambda+b)\left(\lambda+b\frac{P}{\bar{P}}\right)\left\{\lambda^3+\left(P+\frac{P}{\bar{P}}+1\right)\lambda^2 \qquad (14)$$

$$+P\left(\frac{P}{\bar{P}}\bar{r}-r+1+\frac{1}{\bar{P}}+\frac{P}{\bar{P}}\right)\lambda \qquad (15)$$

$$-\left(\frac{P^2}{\bar{P}}\right)[(1+\langle\delta\rangle)r-\bar{r}-1]\right\}=0. \qquad (16)$$

In this way, a perfect agreement with the results of the linear theory previously obtained [see Eqs. (2)] is achieved. Indeed, X_O is stable if and only if

$$(1+\langle\delta\rangle)r-\bar{r}<1, \qquad (17)$$

$$\frac{\bar{P}^2}{(P+\bar{P})(1+\bar{P})}\left[1+\frac{1}{(1+P)}\left(\frac{P}{\bar{P}}\right)\langle\delta\rangle\right]r$$
$$-\frac{P^2}{(P+\bar{P})(1+P)}\bar{r}<1.$$

Note that positions of the stationary states (6) and (7), as well as domains (11) and (12), depend on β_ϵ which is non-continous when the sign of the temperature difference across upper and lower plates changes, namely, $\Delta T\to0$. Accordingly, $\beta_1-\beta_{-1}=2[1+(P/\bar{P})]$ (or, equivalently, $(\partial\beta_\epsilon/\partial\Delta T)_{\Delta T=0}=2[1+(P/\bar{P})]\delta(\Delta T)$). Such a property could be an interesting issue left for future work.

III. INTERMITTENCY IN CHAOTIC DYNAMICAL SYSTEMS

In this section we shall review some basic mathematical definitions and concepts on sensitive dependence on initial conditions, which will be employed in Sec. IV. Let us consider a dynamical system in R^N defined by the set of equations

$$\dot{X}_i=f_i(X_1,\ldots,X_N), \quad i=1,\ldots,N. \qquad (18)$$

An infinitesimal disturbance $\delta X(t)$ evolves according to

$$\delta\dot{X}_i(t)=J_{ij}(t)\delta X_j(t) \quad \text{with} \quad J_{ij}(t)=\frac{\partial f_i}{\partial X_j}\Bigg|_{X=X(t)}. \qquad (19)$$

We can define the response function $R(t,0)$ as

$$R(t,0)=\frac{|\delta X(t)|}{|\delta X(0)|}. \qquad (20)$$

The Oseledec theorem [25] tell us that, for $t\to\infty$ and for almost all (in the sense of measure theory) initial conditions $\delta X(0)$, we have

$$R(t,0)\to e^{\lambda_1 t}, \qquad (21)$$

where λ_1 is called the *maximum Lyapunov exponent* [26]. Naively, one may guess that λ_1^{-1} is the only characteristic time scale of the error growth.

Considering times sufficiently long to have an exponential growth rate for the response function $R(t,0)$, we can write

$$R(t,0) \sim e^{\gamma t}, \qquad (22)$$

where γ is the *local* error growth exponent, in the sense that it depends on the particular initial condition under consideration. Due to fluctuations on γ [27,28], even assuming that t is large enough to observe an exponential growth rate of $R(t,0)$, λ_1^{-1} is not the only relevant time scale: depending on initial conditions, dynamical systems can show, on an empirical basis, states or configurations which can be predicted for time longer or shorter than λ_1^{-1}.

Following Paladin and Vulpiani [29], Benzi and Carnevale [30] and Benzi *et al.* [31], in order to capture information on the large fluctuations in $R(t,0)$, let us introduce the moments

$$\langle R(t,0)^q \rangle, \qquad (23)$$

where $\langle \ \rangle$ is the average over different initial conditions.

If many times scales characterize the error growth, we should have

$$\langle R(t,0)^q \rangle \sim e^{L(q)t}, \qquad (24)$$

with $L(q)$ a nonlinear function of q. The $L(q)$'s are the so called *generalized Lyapunov exponents* [32,33]. As an example, let us consider the simple one-dimensional ''tent map'' [20]

$$X_{n+1} = \begin{cases} \dfrac{X_n}{c} & (0 \leq X \leq c) \\[2mm] \dfrac{1-X_n}{1-c} & (c < X \leq 1), \end{cases} \qquad (25)$$

where $c \in [0,1]$ is the parameter which characterizes the two different (if $c \neq 1/2$) slopes of the map.

It is easy to verify [31] that the expression for $L(q)$ reads

$$L(q) = \ln[c^{1-q} + (1-c)^{1-q}]. \qquad (26)$$

For c close to zero, the error growth of the system can be either in the ''fast'' state (if $X \in [0,c]$), or in the ''slow'' state (if $X \in [c,1]$). Thus $L(q)$ is no longer characterized by a single time scale. Notice that the situation changes when $c = 1/2$. In this case, the map has only one slope, and Eq. (26) reduces to

$$L(q) = q\lambda_1, \qquad (27)$$

with $\lambda_1 = \ln 2$. Relation (27) means that λ_1 is the only relevant time scale characterizing the error growth.

Coming back to the general case, we can rewrite $R(t,0)$ as

$$R(t,0) = \prod_{i=1}^{M} R(t_i, t_{i-1}), \qquad (28)$$

where $0 = t_0 < t_1 < \cdots < t_i < t_{i+1} < \cdots < t_M = t$. Here we view the trajectory as a sequence of M trajectories. By introducing the notation

$$R(t_i, t_{i-1}) \sim e^{\gamma_i(t_i - t_{i-1})}, \qquad (29)$$

we have

$$e^{\gamma t} = e^{\sum_{i=1}^{M} \gamma_i(t_i - t_{i-1})}. \qquad (30)$$

Therefore, taking $t_i - t_{i-1} = \Delta t$ for any i, we have $t = M\Delta t$ and

$$\gamma = \frac{1}{M} \sum_{i=1}^{M} \gamma_i. \qquad (31)$$

Let $P_M(\gamma)$ be the probability of having γ at the time $t = M\Delta t$. The quantity $\langle R(t,0)^q \rangle$ can be computed by the integral

$$\langle R(t,0)^q \rangle = \int P_M(\gamma) e^{\gamma q M \Delta t} d\gamma. \qquad (32)$$

It is now clear that, for $M \to \infty$, $P_M(\gamma) \to \delta(\gamma - \lambda_1)$. For finite M, the theory of large deviations (for a general exposition see Varadhan [34] and Ellis [35]) suggests that

$$P_M(\gamma) \sim e^{-S(\gamma) M \Delta t}, \qquad (33)$$

where $S(\gamma) \geq 0$ and $S(\gamma) = 0$ for $\gamma = \lambda_1$. In the language of large deviation theory, $S(\gamma)$ is called *Cramer function* or *Cramer entropy*. For a description of the link with the statistical mechanics formalism, see Refs. [29,31,33].

Equation (33) can be rigorously proved to be valid in many cases. Inserting Eq. (33) into Eq. (32), by saddle-point integration we obtain

$$\langle R(t,0)^q \rangle \sim \int e^{[\gamma q - S(\gamma)] M \Delta t} d\gamma \sim e^{L(q) M \Delta t}, \qquad (34)$$

where

$$L(q) = \sup_\gamma [q\gamma - S(\gamma)]. \qquad (35)$$

It follows from Eq. (35) that, for any q, a value γ_q exists such that

$$\left. \frac{dS(\gamma)}{d\gamma} \right|_{\gamma = \gamma_q} = q. \qquad (36)$$

Thus

$$L(q) = q\gamma_q - S(\gamma_q) \qquad (37)$$

and

$$\frac{dL(q)}{dq} = \gamma_q + q \frac{d\gamma_q}{dq} - \frac{dS(\gamma_q)}{dq} = \gamma_q. \qquad (38)$$

From Eq. (37), we deduce that, for $q = 0$, $\gamma_0 = \lambda_1$; therefore from Eq. (38) it follows that

$$\lambda_1 = \left. \frac{dL(q)}{dq} \right|_{q=0}. \qquad (39)$$

The quantities γ_q are the characteristic time scales describing the predictability fluctuations of the dynamical system.

There is no general theory about the shape of the $S(\gamma)$ function, as different systems may have different predictability fluctuations.

Let us consider the response function

$$R(t,t') = \frac{|\delta X(t')|}{|\delta X(t)|}, \tag{40}$$

and observe that it obeys the multiplicative rule

$$R(t,t') = R(t,t'')R(t'',t') \tag{41}$$

for any t''. Thus, in order to look for a parametrization of $P_t(\gamma)$, one is led to consider all possible probability functions $P_t(\gamma)$ which are left invariant with respect to the multiplicative transformation (41). In the following, we shall call this class of probability functions *covariant*. By making the strong assumption of weak correlation between $R(t,t'')$ and $R(t'',t')$, an important category of distributions turn out to be covariant: it is the class of the *infinitively divisible distributions* (IDD's) [36].

A. Gaussian case

The Gaussian distribution is the most popular examples of IDD's. The idea of using IDD's is closely connected to similar studies performed in the framework of the statistical theory of turbulence [37] and of the theory of atmospheric predictability [31].

A Gaussian law for $P_t(\gamma)$ means a quadratic shape for $S(\gamma)$ [29]

$$S(\gamma) = (\gamma - \lambda_1)^2/2\mu, \tag{42}$$

and a log-normal distribution for the response function $R(t,0)$,

$$P_t(R) = \frac{1}{R\sqrt{2\pi\mu t}} e^{-[(\ln R - \lambda_1 t)^2/2\mu t]}. \tag{43}$$

In this case, the probability distribution is fully characterized by only two parameters:

$$\lambda_1 = \langle \ln R(t,0) \rangle/t, \tag{44}$$

$$\mu = [\langle (\ln R(t,0))^2 \rangle - \langle \ln R(t,0) \rangle^2]/t,$$

where λ_1 is the maximum Lyapunov exponent, and μ is the second cumulant, called *intermittency* .

The moments of the distribution (43) give

$$L(q) = \lambda_1 q + \tfrac{1}{2}\mu q^2, \tag{45}$$

while the most probable value of the response function and the mean value are, respectively,

$$\widetilde{R} = e^{\lambda_1 t(1-\mu/\lambda_1)}, \quad \langle R \rangle = e^{\lambda_1 t[1+\mu/(2\lambda_1)]}. \tag{46}$$

Arguments reported by Crisanti *et al.* in Ref. [38] show that the predictability problem is reduced to a "first exit problem." Relations between the probability distribution function
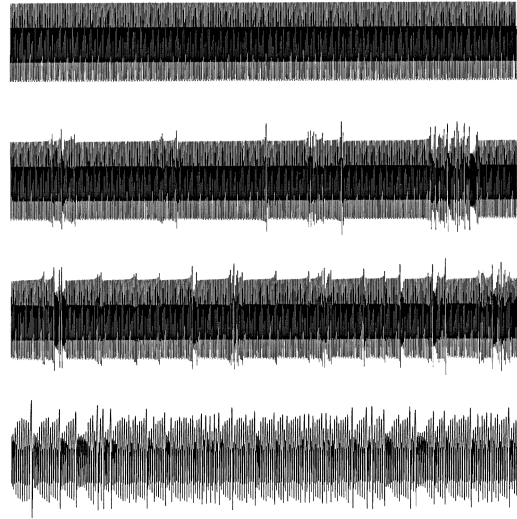
FIG. 1. Time record of the X_5 coordinate in the five-mode Lorenz model (5). (a) Stable periodic motion appears for $\langle \delta \rangle$ (here ~ 0.096) just above threshold $\langle \delta \rangle_c \sim 0.0955$. (b) Just below $\langle \delta \rangle_c$ ($\langle \delta \rangle \sim 0.095$) the regular oscillations are "randomly" interrupted by chaotic "bursts" which become more frequent as $\langle \delta \rangle$ is decreased [case (c) with $\langle \delta \rangle \sim 0.093$]. In the thermohaline convection (d), i.e., $\langle \delta \rangle = 0$, the system behaves chaotically during all the observed time. The X_5 coordinate is ranging between -72 and -23 while the dimensionless time between 10885 and 11235 in all cases (linear scales).

of the predictability time, and fluctuations of the local Lyapunov exponent γ, are proposed there by the authors.

A further way to take into account the effects of fluctuation was recently proposed by Benzi *et al.* in Ref. [31], in the framework of the theory of atmospheric predictability. Following Ref. [31], a reasonable definition of the characteristic predictability time τ of the system, which takes into account the effects of fluctuations, can be given as

$$\tau \sim \frac{1}{L(1)} = \frac{1}{\lambda_1 + (1/2)\mu}, \tag{47}$$

which will turn out to be useful in the following when the system behavior near a bifurcation intermittency will be investigated. A deep discussion on the reliability of the log-normal approximation can be found elsewhere [29], and thus will not be reported here.

IV. INTERMITTENCY ROUTE TO CHAOS DRIVEN BY THE TRANSVERSE EFFECT

For nonlinear dissipative dynamical systems, there are different well defined [39] patterns of behavior ("scenarios"), as the system is driven from stable laminar motion into chaotic motion. In this section we present the results of some numerical experiments performed on the five-mode Lorenz model (5). In our experiments, where the external control parameter is just the cross-term $\langle \delta \rangle$, the intermittency routes to chaos originally proposed for the $L63$ model by Manneville and Pomeau [19] will be evidenced. All numerical integrations were made by using a fourth-order Runge-Kutta scheme with $\Delta t = 0.005$. Figure 1 shows the time dependence of X_5 (a similar behavior is observed for the other
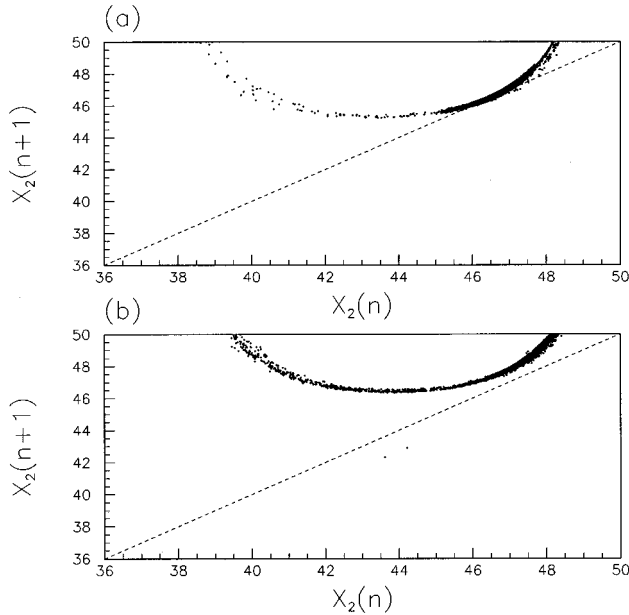
FIG. 2. An expanded view of the Poincaré map along the X_2 coordinate. Case (a) corresponds to the intermittency transition when $\langle\delta\rangle=\langle\delta\rangle_c$ while (b) is relative to $\langle\delta\rangle$ values slightly beyond the intermittency threshold $\langle\delta\rangle_c$. Note that at the transition the "curve" is tangent to the diagonal line, while a small gap ("channel") appears for $\langle\delta\rangle$ slightly below $\langle\delta\rangle_c$. Here, a trajectory spends a significant amount of time. The motion along the channel represents the phase of the laminar motion.

$X_{i\neq5}$) when four different values of the control parameter $\langle\delta\rangle$ are considered, and when the r parameter is 167. The other model parameters (kept fixed in the present study) are $\bar{r}=50$, $\epsilon=1$ and $\bar{\epsilon}=-1$, corresponding to a thermodiffusive convection with opposite temperature and concentration gradients. Moreover, for the sake of simplicity, on investigating the thermal cross-contribution in the limit of a gaslike behavior, the Prandtl and Schmidt numbers were setted to $P=8$ and $\bar{P}=10$.

Above the critical value, which turned out to be $\langle\delta\rangle_c\sim0.0955$, numerical simulations show regular periodic oscillations [see Fig. 1(a)]; for $\langle\delta\rangle$ slightly below $\langle\delta\rangle_c$ the system appears to switch from periodic to chaotic behavior [see Fig. 1(b)]. As $\langle\delta\rangle$ decreases [see Fig. 1(c)], the time spent in chaotic motion increases, while the duration of the periodic stages decreases, until the model behaves completely chaotically. This corresponds to $\langle\delta\rangle=0$ [see Fig. 1(d)], i.e., to the thermohaline regime [10].

Since the bifurcation event can be tangent or saddle node, such a type of intermittency route to chaos is sometimes called *tangent bifurcation intermittency*. It has been observed during many experiments (see, for example, Jeffries and Perez [40]), particularly when the focused system also shows the period-doubling route to chaos.

To analyze the behaviors reported in Fig. 1, following Manneville and Pomeau [19] consider the Poincaré map defined as $X_2(n+1)=g[X_2(n),\langle\delta\rangle]$, $X_2(n)$ being the X_2 coordinate at the nth crossing of the plane $X_1=0$, and endowed with the condition $\dot{X}_1>0$. After performing numerical simulations on model (5), the resulting map is shown in an ex-
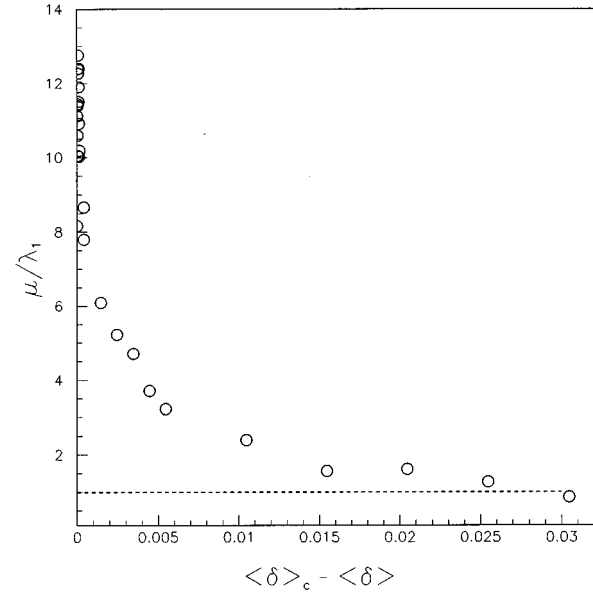
FIG. 3. Behavior of the ratio μ/λ_1, vs the displacement from the intermittency threshold $\langle\delta\rangle_c=0.0955$. Notice the transition, for $\langle\delta\rangle\gtrsim0.065$, from weak ($\mu/\lambda_1<1$) to strong ($\mu/\lambda_1>1$) intermittency.

panded view in Fig. 2. It can be seen that, for $\langle\delta\rangle=\langle\delta\rangle_c$ the "curve" is just tangent to the diagonal line [see Fig. 2(a)], while for $\langle\delta\rangle<\langle\delta\rangle_c$ [see Fig. 2(b)] the curve is lifted up and a "channel" appears. The graphic iteration technique shows that a trajectory spends a significant amount of time traveling along the channel. Such a time corresponds to the laminar phase of the motion illustrated both by Figs. 1(b) and 1(c).

Based on the use of a renormalization (scaling) argument [21] it is possible to determine the average periodic burst duration according to small values of the difference $\langle\delta\rangle_c-\langle\delta\rangle$. As a result, the scaling argument gives a number of iterations, and therefore a characteristic "predictability time" τ of the order of

$$\tau\sim(\langle\delta\rangle_c-\langle\delta\rangle)^{-1/2}, \qquad (48)$$

which is necessary to cross the channel.

Near the critical points $\langle\delta\rangle_c$, the influence of fluctuations is strong. This can be concluded from Fig. 3, where the ratio between the maximum Lyapunov exponent λ_1 and the intermittency μ [see Eqs. (44)] is evaluated when the control parameter $\langle\delta\rangle$ approaches the critical point $\langle\delta\rangle_c=0.0955$. As one can see, when $\langle\delta\rangle\gtrsim0.065$ a transition from $\mu/\lambda_1<1$ to $\mu/\lambda_1>1$, i.e., from weak to strong intermittency, occurs. The word "transition" is used, in this context, in a broader sense than elsewhere, when the tangent bifurcation has been discussed. Even variations in the chaoticity degree, which implies $\mu/\lambda_1>1$, are included in the class of intermittent behaviors [29].

Recalling definitions (46) for the most probable value $\widetilde{R}$ and the mean value $\langle R\rangle$, taking $\widetilde{R}$ as representative of the distribution turns out to be inadequate for $\langle\delta\rangle\gtrsim0.065$. In fact, instead of the turbulent chaotic regime, characterized by a positive exponent ($\lim_{t\to\infty}\langle R\rangle=\infty$), a laminar stable phase ($\lim_{t\to\infty}\widetilde{R}=0$) is predicted. In the phase transition jargon this means that the mean field picture fully breaks down. Chaotic behavior near a bifurcation intermittency is thus no
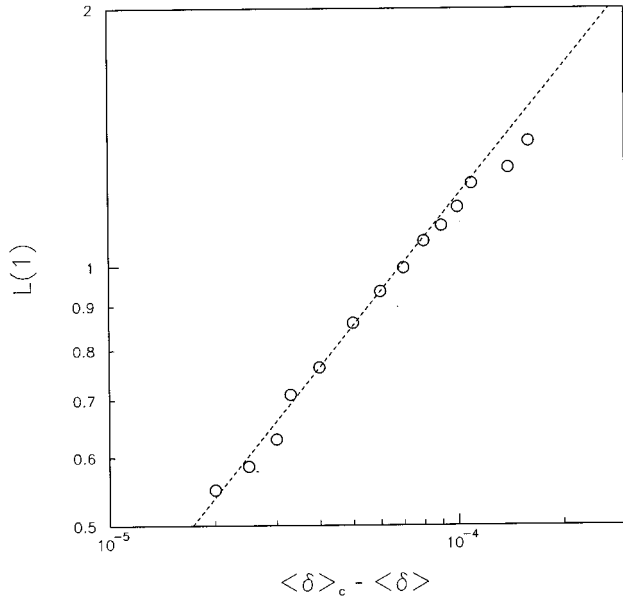
FIG. 4. Generalized Lyapunov exponent behavior, $L(1)$, vs the displacement from the intermittency threshold $\langle\delta\rangle_c=0.0955$. Notice that the predicted scaling law $L(1)\sim(\langle\delta\rangle_c-\langle\delta\rangle)^{1/2}$ (dashed line) closely agrees with the numerical simulations (circles), which is affected by a relative uncertainty of about 8%.

longer characterized by the sole Lyapunov exponent. The effect of fluctuations is important, and must be taken into account to characterize accurately the model predictability. As a definition of the characteristic predictability time τ which reasonably takes into account the influence of fluctuations, consider formula (47). In the intermittent region, it follows from Eq. (48) that the generalized Lypaunov exponent $L(1)$ should vary as

$$L(1)\sim(\langle\delta\rangle_c-\langle\delta\rangle)^{1/2}. \qquad (49)$$

$L(1)$ is plotted in Fig. 4 versus the displacement from the intermittency threshold $\langle\delta\rangle_c=0.0955$. As one can verify, in a range of $\langle\delta\rangle$ values just below $\langle\delta\rangle_c$, the scaling law for $L(1)$ given by Eq. (49) (dashed line) is consistent with the $L(1)$ behavior obtained by performing numerical simulations of the deterministic model (5). Evaluation of $L(1)$ is done by determining λ_1 and μ through a linear least-square fit of $\langle\ln R(t,0)\rangle$ and $\langle(\ln R(t,0))^2\rangle-\langle\ln R(t,0)\rangle^2$ versus t, respectively.

Small deviations from theoretical predictions can be attributed to the slow convergence of the μ indicator at the intermittency threshold. The relative errors generated in the fits is of the order of 8%.

We conclude by observing that, when the transverse Soret coefficient is used as a control parameter, routes to chaos via tangent bifurcations intermittency seem to be a quite common feature, in a wide range of r-parameter values. Intermittency routes to chaos via tangent bifurcation intermittency occur in fact not only for large values of r (as it is the case with the $L63$ model; see Ref. [19]). For instance, we have identified other tangent bifurcations for $r=38$ (the other parameters are kept unchanged with respect to the case already discussed) when the control parameter $\langle\delta\rangle$ is ~0.7222 and ~0.9799, respectively.

V. CONCLUSIONS

(1) Intermittent chaos in a five-mode truncated model has been studied in a gaseous binary system endowed with transverse (Soret $\langle\delta\rangle$) coefficient in a nonstationary state for the mass transfer. Accordingly, we have the following.

(i) From performed numerical experiments, when the external control parameter $\langle\delta\rangle$ approaches some critical values $\langle\delta\rangle_c$, one can observe routes to chaos as proposed by Manneville and Pomeau [19] for the $L63$ model. The transition occurring when $\langle\delta\rangle_c\sim0.0955$, and when the reduced Rayleigh number $r\sim167$, were reported. The system also exhibited the tangent bifurcation intermittency when r assumed smaller values. As an example, for $r\sim38$, we identified two critical points $\langle\delta\rangle_c\sim0.7222$ and 0.9799, respectively.

(ii) Fluctuations in the chaotic behavior near the bifurcation at $\langle\delta\rangle_c\sim0.0955$ have been detected, and a neighborhood inside the chaotic zone where the mean field picture fully breaks down has been recognized. Then, correspondingly, the influence of fluctuations on the chaotic behavior must necessarily be accounted for. It must be concluded that, in such a region, the Lyapunov exponent is not sufficient for characterizing chaos and predictability time exhaustively. Generalized Lyapunov exponents $L(q)$ have been employed to define coherently the predictability time as depending on fluctuation effects.

(iii) The inverse predictability time, i.e., $L(1)$, vs displacement from the critical point $\langle\delta\rangle_c\sim0.0955$ has been derived numerically and compared with theoretical scaling-law-based results. Numerical simulations reasonably agree with theoretical predictions.

(2) The analysis of linear stability and stationary states, applied to the model, provided results in agreement with those of classical hydrodynamic (marginal locus of stability). All stationary states and stability regions have been derived parametrically (in $r,\bar{r},P,\bar{P}$ and $\langle\delta\rangle$). A term which is not continuous when the sign of the temperature gradient is changed has also appeared.

ACKNOWLEDGMENTS

APPENDIX A: REMARKS ON THE MARGINAL LOCUS OF STABILITY IN THE THERMO-SOLUTAL CONVECTION

We considered a linear theory developed in normal modes, as obtained when ideal boundary conditions are adopted: free, conducting, permeable, and indefinitely extended surfaces (if the layer thickness is not too thin, the Marangoni effect can be ignored [41,42]). Moreover,

$$\Gamma(\boldsymbol{r},t)=\int\bar{\Gamma}_{\boldsymbol{k}}(z,t)e^{i\boldsymbol{k}\cdot\boldsymbol{r}}d\boldsymbol{k}, \qquad (A1)$$

$$\bar{\Gamma}_{\boldsymbol{k}}(z,t)=\hat{\Gamma}_{\boldsymbol{k}}(z)e^{i\omega_{\boldsymbol{k}}t}, \qquad \omega_{\boldsymbol{k}}\in\mathcal{C}$$

were the general Fourier developments for the infinitesimal disturbances (velocity components, temperature, and concentration perturbations), where $r \equiv (x,y)$ and $k \equiv (k_x, k_y)$ is the relative bidimensional wave number.

The linear theory of stability applied to perturbations (A1) yields the criteria to predict the stable-to-unstable transition of the system being considered. In the Bénard problem, it is well known [43,44] that, for a given adimensional wave number $\alpha = (k_x^2 + k_y^2)^{1/2} d$, where d is the layer thickness, we have stability if and only if $R < R_1(\alpha) = (\pi^2 + \alpha^2)^3 / \alpha^2$, where $R_1(\alpha)$ is the ''marginal stability'' locus point, and $R = g a \alpha_P d^4 / \nu \chi$ is the Rayleigh number. It follows that the critical Rayleigh number R_c, expected to produce instability, is given by $R_c = \min_\alpha \{R_1(\alpha)\} = \frac{27}{4} \pi^4$, when $\alpha = \alpha_c = 2^{-1/2} \pi$. The quantity R contains the gravity constant g, the temperature gradient $a = \Delta T / d$ (positive, in the adopted convention, if the fluid is heated from below), the expansivity coefficient α_P, the kinematic viscosity ν, the thermal diffusivity χ, and the layer thickness d.

The study of the stability of a fluid layer solely subject to a concentration gradient [45] shows an identical criterion for a solutal number $\bar{R}$ (here defined in the following) which replaces the Rayleigh number. It is also known that in the thermohaline convection, i.e., in a binary fluid subject to independent temperature and concentration gradients and to ''ideal'' (conductive and permeable) boundary conditions, one has stability if and only if [2,7,10]

$$R - \bar{R} = \frac{27}{4} \pi^4, \qquad (A2)$$

$$\frac{\bar{P}^2}{(\bar{P}+P)(1+\bar{P})} R - \frac{P^2}{(\bar{P}+P)(1+P)} \bar{R} = \frac{27}{4} \pi^4,$$

where $\alpha = \alpha_c = 2^{-1/2} \pi$ again and $\bar{R} = g b \gamma_m d^4 / \nu D$ is the solutal (Rayleigh) number; it contains the concentration gradient $b = \Delta c / d$ (negative if the solute is denser at the upper surface), while $\gamma_m = \rho_0^{-1} (\partial \rho / \partial c_1)_{T,P}$ is defined in the development of the density function $\delta \rho = \rho_0 (1 - \alpha_P \delta T + \gamma_m \delta c_1)$. The quantities $P = \nu / \chi$ and $\bar{P} = \nu / D$ are the Prandtl and Schmidt numbers, respectively.

APPENDIX B: DISCUSSION OF THE STATIONARY SOLUTION

The stationary solutions of thermohaline convection-based equations depend on the involved physical parameters and, with regard to Eqs. (A1), for any fixed values of k and t, one has

$$\bar{\Gamma}_k \propto \hat{\Gamma}_k(P, \bar{P}; \epsilon, \bar{\epsilon}, R, \bar{R},) = \hat{\Gamma}_k^*(\chi, \nu, D; T_0, T_d, c_0, c_d, d). \qquad (B1)$$

The function $\bar{\Gamma}_k$ depends on the sign of the temperature gradient ΔT and on the concentration gradient Δc_1. In $\hat{\Gamma}_k^*$ are explicitly included not only ΔT and Δc_1, as requested by the dependence of R on ΔT and of $\bar{R}$ on Δc_1, but also the boundary values T_o, T_d, c_o, and c_d (o indicates the lower plane, while d indicates the upper plane).

With the Soret effect, two further parameters S_T and $\tilde{c}_1$ must be introduced; accordingly,

$$\bar{\Gamma}_{kz} \propto \hat{\Gamma}_{kz}(P, \bar{P}, S_T; \epsilon, \bar{\epsilon}, R, \bar{R}, \tilde{c}_1)$$
$$= \hat{\Gamma}_{kz}^*(\chi, \nu, D, D'; T_0, T_d, c_0, c_d, d), \qquad (B2)$$

where the symbol z indicates a fixed z: $\tilde{c}(z) = c_0 - bz = c_0 - [(c_0 - c_d)/d]z$. Now, with the change of units $\tilde{c}_1 \to \tilde{C}_1$, the dependence of $\hat{\Gamma}_{kz}$ on all parameters changes, i.e., $\hat{\Gamma}_{kz} \to \widetilde{\Gamma_{kz}}$, but $\hat{\Gamma}_{kz}^*$ remains unchanged, namely,

$$\hat{\Gamma}_{kz} \to \widetilde{\hat{\Gamma}}_{kz}(P, \bar{P}, S_T; \epsilon, \bar{\epsilon}, R, \bar{R}, \tilde{C}_1)$$
$$\equiv \hat{\Gamma}_{kz}^*(\chi, \nu, D, D'; T_0, T_d, c_0, c_d, d). \qquad (B3)$$

Accordingly, the application of the linear theory [13,24] to derive the stability conditions must be subject, for any unity change, to constraint (8).

APPENDIX C: REMARKS ON LORENZ-BASED TRUNCATED MODELS

All Lorenz truncated models follow from Saltzman bidimensional equations, in which the convective terms are considered [22,46]. Choosing, for instance, the x and z coordinates, and introducing the stream function ψ in such a way as to preserve the continuity equation in the (x,z) plane, they are [11]

$$\frac{\partial \nabla^2 \psi}{\partial t} = -\{\psi, \nabla^2 \psi\}_{xz} + g\left(\alpha_P \frac{\partial \theta}{\partial x} - \gamma_m \frac{\partial \xi}{\partial x}\right) + \nu \nabla^4 \psi,$$

$$\frac{\partial \theta}{\partial t} = -\{\psi, \theta\}_{xz} + a \frac{\partial \psi}{\partial x} + \chi \nabla^2 \theta, \qquad (C1)$$

$$\frac{\partial \xi}{\partial t} = -\{\psi, \xi\}_{xz} + b \frac{\partial \psi}{\partial x} + D \nabla^2 \xi + (\tilde{c}_1 + \xi)$$
$$\times (1 - \tilde{c}_1 - \xi) D' \nabla^2 \theta,$$

where t is the time, θ is the temperature perturbation, and ξ and $\tilde{c}_1$ are the concentration gradient and the vertical linear concentration profile at the stationary state, respectively; also, $\nabla^4 * = \nabla^2 \cdot (\nabla^2 *)$, and having introduced the Jacobi determinant, $\{f, g\}_{xz} \triangleq (\partial f / \partial x)(\partial g / \partial z) - (\partial f / \partial z)(\partial g / \partial x)$.

If one supposes that the spatial parts of ψ, θ and ξ, which have to be determined, are developable in Fourier double series with nondimensional and time-dependent complex coefficients, namely,

$$\bar{\psi}(\mathcal{X}, \mathcal{Z}, \bar{t}) = \sum_{m,n=-\infty}^{+\infty} \bar{\Psi}_{m,n}(\bar{t}) e^{i(m\alpha\mathcal{X} + n\pi\mathcal{Z})},$$

$$\bar{\theta}(\mathcal{X}, \mathcal{Z}, \bar{t}) = \sum_{m,n=-\infty}^{+\infty} \bar{\Theta}_{m,n}(\bar{t}) e^{i(m\alpha\mathcal{X} + n\pi\mathcal{Z})}, \qquad (C2)$$

$$\bar{\xi}(\mathcal{X}, \mathcal{Z}, \bar{t}) = \sum_{m,n=-\infty}^{+\infty} \bar{\Gamma}_{m,n}(\bar{t}) e^{i(m\alpha\mathcal{X} + n\pi\mathcal{Z})},$$

the Galerkin procedure can be applied to Eqs. (C1) and (C2). In developments (C2), $\bar{\psi}=\psi/\chi$, $\bar{\theta}=R\,\theta/|\Delta\widetilde{T}|$, $\bar{\xi}=\bar{R}\,\xi/|\Delta\widetilde{c}_1|$, $\mathcal{X}=x/d$, $\mathcal{Z}=z/d$, and $\bar{t}=(\pi^2+\alpha^2)\chi t/d^2$ are nondimensional quantities, and $\Delta\widetilde{T}\equiv ad$ and $\Delta\widetilde{c}_1\equiv bd$ are the differences in temperature and concentration of the boundaries at mechanical equilibrium; further, we set [11,46] $\bar{\Psi}_{m,n}(\bar{t})=\bar{\Psi}^{(1)}_{m,n}(\bar{t})-i\bar{\Psi}^{(2)}_{m,n}(\bar{t})$, $\bar{\Gamma}_{m,n}(\bar{t})=\bar{\Gamma}^{(1)}_{m,n}(\bar{t})-i\bar{\Gamma}^{(2)}_{m,n}(\bar{t})$, and $\bar{\Theta}_{m,n}(\bar{t})=\bar{\Theta}^{(1)}_{m,n}(\bar{t})-i\bar{\Theta}^{(2)}_{m,n}(\bar{t})$.

---

[1] S. R. De Groot and P. Mazur, *Nonequilibrium Thermodynamics* (North-Holland, Amsterdam, 1963).

[2] P. Glansdorff and I. Prigogine, *Thermodynamic Theory of Structure Stability and Fluctuations* (Wiley-Interscience, New York, 1971).

[3] J. R. Manning, *Diffusion Kinetics for Atoms in Crystal* (Van Nostrand, Princeton, 1968).

[4] P. W. Bridgman, *The Thermodynamics of Electrical Phenomena in Metals and a Condensed Collection of Thermodynamic Formulas* (Dover, New York, 1961).

[5] P. G. Shewman, *Diffusion in Solids* (McGraw-Hill, New York, 1963).

[6] P. M. Capurro, and S. A. Mezzasalma (unpublished); A. Capecchi and M. Capurro, J. Phys. (Paris), Colloq. **44**, C9-447 (1983).

[7] D. T. J. Hurle and E. Jakeman, J. Fluid Mech. **47**, 667 (1971).

[8] J. C. Legros, J. K. Platten and P. G. Poty, Phys. Fluids **15**, 1383 (1972); S. J. Linz and M. Lucke, *ibid.* **36**, 3505 (1987).

[9] D. T. J. Hurle and E. Jakeman, Phys. Fluids **12**, 2704 (1969).

[10] R. S. Schechter, M. G. Velarde, and J. K. Platten, Adv. Chem. Phys. **26**, 256 (1974).

[11] J. K. Platten and J. C. Legros, *Convection in Liquid* (Springer-Verlag, Berlin, 1984).

[12] R. S. Schechter, I. Prigogine, and J. R. Hamm, Phys. Fluids **15**, 379 (1972).

[13] L.E. Reichl, *A Modern Course in Statistical Physics* (Arnold, Sevenoaks, UK, 1980).

[14] E. Knobloch and D. R. Moore, Phys. Rev. A **37**, 860 (1988).

[15] K. Kaneko, Prog. Theor. Phys. **74**, 1033 (1995).

[16] H. Chaté and P. Manneville, Phys. Rev. A **38**, 4351 (1988).

[17] H. Chaté and P. Manneville, Physica D **32**, 409 (1989).

[18] T. Bohr, M. H. Jensen, G. Paladin, and A. Vulpiani, *Dynamical Systems Approach to Turbulence* (Cambridge University Press, Cambridge, in press).

[19] P. Manneville and Y. Pomeau, Physica D **1**, 219 (1980).

[20] R.C. Hilborn, *Chaos and Nonlinear Dynamics* (Oxford University Press, New York, 1994).

[21] J. Guckenheimer and P. Holmes, *Nonlinear Oscillations, Dynamical Systems, and Bifurcations of Vector Fields*, 3rd ed. (Springer-Verlag, New York, 1990).

[22] E. N. Lorenz, J. Atmos. Sci. **20**, 130 (1963).

[23] W.F. Ames, *Nonlinear Partial Differential Equations in Engineering* (Academic, New York, 1965).

[24] J. L. McCauley, Phys. Scr. **T20**, 6 (1988).

[25] V. I. Oseledec, Trans. Moscow Math. Soc., **19**, 197 (1968).

[26] G. Benettin, L. Galgani, A. Giorgilli, and J. M. Strelcyn, Meccanica **9**, 15 (1980); **15**, 21 (1980).

[27] J. P. Eckmann and I. Procaccia, Phys. Rev. A **34**, 659 (1986).

[28] G. Paladin, L. Peliti, and A. Vulpiani, J. Phys. A **19**, L991 (1986).

[29] G. Paladin and A. Vulpiani, Phys. Rep. **156**, 147 (1987).

[30] R. Benzi and G. Carnevale, J. Atmos. Sci. **46**, 3595 (1989).

[31] R. Benzi, M. Marrocu, A. Mazzino, and E. Trovatore (unpublished).

[32] H. Fujisaka, Prog. Theor. Phys. **70**, 1264 (1983).

[33] R. Benzi, G. Paladin, G. Parisi, and A. Vulpiani, J. Phys. A **18**, 2157 (1985).

[34] S. R. S. Varadhan, *An Introduction to the Theory of Large Deviations* (Springer-Verlag, Berlin, 1984).

[35] R. S. Ellis, *Entropy, Large Deviations and Statistical Mechanics* (Springer-Verlag, Berlin, 1985).

[36] J. L. Doob, *Stochastic Processes* (Wiley, New York, 1990).

[37] Z. S. She and E. C. Waymire, Phys. Rev. Lett. **74**, 262 (1995).

[38] A. Crisanti, M. H. Jensen, G. Paladin, and A. Vulpiani, J. Phys. A **26**, 6943 (1993); A. Crisanti, M. H. Jensen, A. Vulpiani, and G. Paladin, Phys. Rev. Lett. **70**, 166 (1993).

[39] J. P. Eckmann, Rev. Mod. Phys. **53**, 643 (1981).

[40] C. Jeffries and J. Perez, Phys. Rev. A **26**, 2117 (1982).

[41] D. A. Nield, J. Fluid Mech. **19**, 341 (1964).

[42] A. N. Garazo and M. G. Velarde, Phys. Fluids A **3**, 2295 (1991).

[43] S. Chandrasekar, *Hydrodynamic and Hydromagnetic Stability* (Clarendon, Oxford, 1961).

[44] F. M. Busse, Rep. Prog. Phys. **41**, 1929 (1978).

[45] F. Gambale and A. Gliozzi, J. Phys. Chem. **76**, 783 (1972).

[46] B. Saltzman, J. Atmos. Sci. **19**, 329 (1961).